CHAPTER 5

CASE STUDIES

In this Chapter, two recent solar eclipses that traversed Southern Africa in relatively short succession, are studied. They occurred on 21 June 2001 and 4 December 2002 and in both cases, a significant portion of the partial phases were visible at De Aar. Both days were clear sky days at De Aar for the entire day, and complete radiation measurements of all basic components without any missing data were possible. The Chapter comprises a short discussion on solar eclipses, followed by (for both eclipses individually), discussions of the path of totality, meteorological background leading to eclipse day, and time-series analysis of the basic radiation components for both eclipses, complemented by comparative tables.

5.1 SOLAR ECLIPSES: BACKGROUND

A solar eclipse is the relatively rare event when the moon in its orbit around the Earth, intercepts the direct line of sight between the Sun and Earth. The resulting shadow (projection of the Moon's umbra) cast on Earth, is called the path of totality. An observer in this narrow strip of land (usually about 200 km wide), will then experience a total solar eclipse. This event lasts theoretically a maximum of 7 minutes and 31 seconds[1], typically only about 1 to 3 minutes, depending on the moon-earth-sun distance ratio. An observer in the adjacent area (a few thousand km wide on both sides), experiences the projection of the Moon's penumbral shadow, i.e., a partial solar eclipse, the magnitude of which is dependant upon the distance from the observation point normal to the path of totality.

Not all solar eclipses have paths of totality. When the moon-earth distance is orientated relative to the sun-earth distance in such a way that an eclipse occurs, but the Earth in space misses the Moon's umbra, the result for an observer on Earth is either a penumbral (partial) eclipse or an annular eclipse. A specific eclipse event can also be hybrid, i.e., a combination of a partial and total eclipse.

[1] http://www.donastro.freeserve.co.uk/tycho.htm

The governing factor of solar eclipses on a temporal scale, the Saros cycle, is in fact an interwoven multitude of simultaneous moon-earth orbit interception cycles waxing and waning over centuries.[2] The period of a Saros cycle is 6585.3215 days (slightly more than 18 years). This is not an exact number of Earth revolutions (days), therefore solar eclipses do not follow exact occurrence in a cycle of days or multiples thereof, but rather seem to be randomly distributed on both a temporal and geographical scale.

For the period 2000 BC to 4000 AD, it has been determined that a total of 14263 eclipses have occurred or are yet to occur[3]. This translates to an average frequency of 2.38 eclipses per year, distributed per eclipse type as listed in Table 5.1:

Table 5.1 *Relative frequency of eclipse types (after NASA's Solar Eclipse Catalogue)*

All eclipses	Total	Partial	Annular	Hybrid
14263 (100 %)	3797 (26.6 %)	5029 (35.3 %)	4699 (32.9 %)	738 (5.2 %)

The last total solar eclipse that traversed South African soil in the 20th century, was on 1 October 1940, followed by the total eclipse of 4 December 2002, while the next total solar eclipse is expected only at 25 November 2030. In the 28 years between the eclipses of 2002 and 2030, there are 61 eclipses expected over the world, of which only 16 will have an impact through its partial phases on South Africa. Therefore, solar eclipses, total or otherwise, over a specific area, such as South Africa, are a relatively rare occurrence that deserve a closer look.

5.2 SOLAR ECLIPSES OVER SOUTHERN AFRICA

Shortly after the establishment of the BSRN site, two total solar eclipses traversed Southern Africa in relatively short succession: one in the winter afternoon of 21 June 2001, and another in the summer morning of 4 December 2002. The path of totality covered Southern Africa in both cases (the latter occurrence slightly further south), with the BSRN site in South Africa being well situated to receive a significant portion of both partial phases.

Comparative figures ref. to events regarding the two eclipses at the De Aar BSRN station, are listed in Table 5.2. All times are quoted in South African Standard Time (SAST), unless stated otherwise. The data was calculated using astronomical software (*www.calsky.com*).

[2] http://sunearth.gsfc.nasa.gov/eclipse/SEsaros/SEsaros.html
[3] http://sunearth.gsfc.nasa.gov/eclipse/SEcat/SEcatalog.html

Table 5.2 *Comparative data at De Aar BSRN station for the 2001 and 2002 eclipses over Southern Africa. Times are in SAST. Note that SAST = UT + 2 hours.*

Event	Eclipse of 21 June 2001	Eclipse of 4 December 2002
Time of sunrise	07:21:00	05:13:42
Time of sunset	17:30:36	19:14:48
Length of day	10:09:36	14:01:06
Time of solar noon	12:25:48	12:14:06
Start of partial phase (first contact)	13:30:34	07:25:09
Time instant of maximum eclipse	14:52:17	08:27:40
Solar elevation angle at maximum eclipse	25.9°	39.5°
Maximum fraction of solar disk obscured	60.7%	73.1%
End of partial phase (fourth contact)	16:04:56	09:37:33

5.3 ECLIPSE OF 21 JUNE 2001

5.3.1 General description

The path of totality for this total solar eclipse is illustrated in a global context in Figure 5.1 and in more detail in Figure 5.2, using a close-up view.

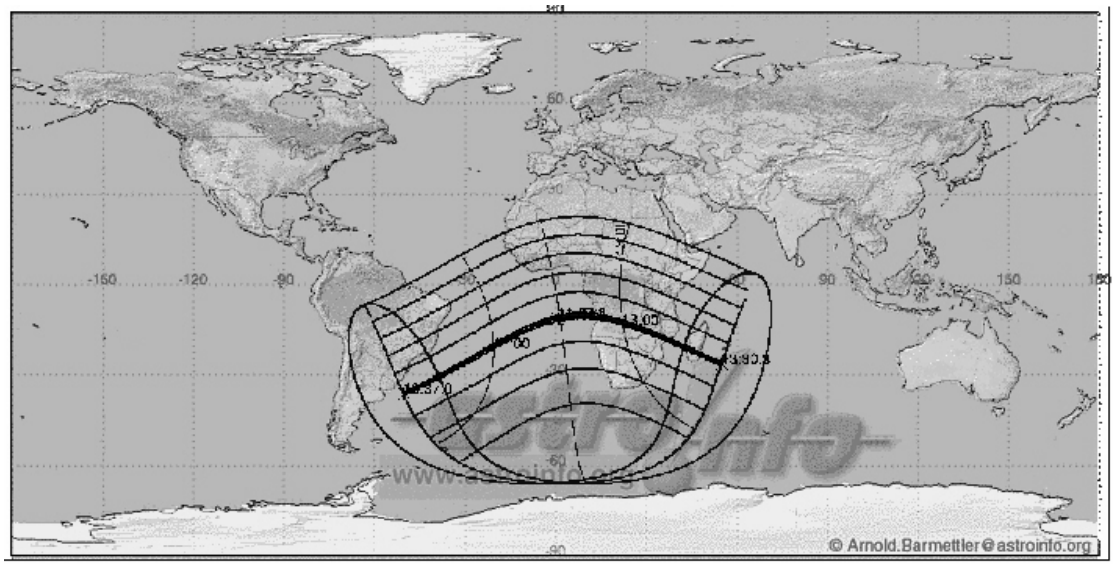

Figure 5.1 *Global orthographic projection of solar eclipse on 21 June 2001. Map by Arnold Barmettler at Astro-Info (www.astro-info.org)*

In Figure 5.1, the path of totality is represented by the thick central line, starting southeast off the Brazilian coast, curving through the Atlantic Ocean, traversing Africa and ending east of Madagascar in the Indian Ocean. The thinner lines parallel to this line respectively represent the 80%, 60%, 40%, 20% and 0% phases, respectively, of the partial eclipse. The dashed line orthogonal to the path of totality, stretching from western Africa along the Atlantic Ocean towards the South Pole, represents the peak line. The intersection between this line and the path of totality west of Angola indicates the eclipse peak at 11°15' S, 02°45' E, where the path of totality had its maximum width (204 km). For an observer at that point, the eclipse occurred at 12:03:42 UT, 105% of the solar disk was obscured and totality would last 5'01".

Since Southern Africa is situated towards the east of the eclipse peak, it experienced the eclipse in the waning phase. Another interesting fact is that the Southern Hemisphere (SH) winter solstice occurred at 07:37:42 SAST, only about 4 hours after the start of the eclipse. The appearance of the eclipse on the shortest day of the year for the SH, was in itself a unique occurrence.

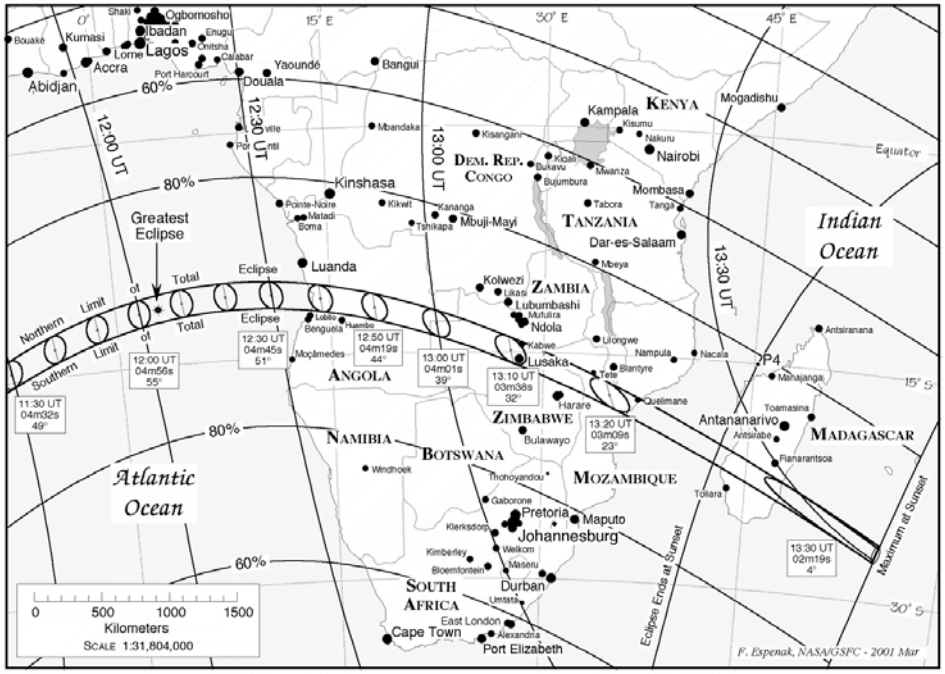

Figure 5.2 *Close up view of 2001 eclipse path through Africa, showing detail of partial phase. Map from Espenak and Anderson (1999). Times in UT*

Figure 5.2 provides a closer view of the eclipse path through Africa, showing details about the partial phases. The totality path entered Africa at the Angolan coast, passing Zambia through the central west, including northern Zimbabwe, southern Zambia and central-west Mozambique as well as the southernmost tip of Malawi. Lusaka in Zambia was the most prominent urban point in Southern Africa under the totality path.

5.3.2 Eclipse in South Africa

In South Africa, partial phase magnitudes were between 51 % at Cape Town, in the extreme Southwest, and up to 80 % at the Kruger National Park in the extreme northeast. Local circumstances for a few major centra in South Africa (Espenak and Anderson, 1999) are listed in Table 5.3.

Table 5.3 *Local circumstances for a few centra in South Africa during eclipse 2001*

Location	Latitude	Longitude	First contact	Last contact	Max eclipse	Magni-tude
Bloemfontein	29°12'S	26°07'E	13:35:21	16:10:21	16:57:45	65.3%
Cape Town	33°55'S	18°22'E	13:17:46	15:49:29	16:36:52	51.3%
Durban	29°55'S	30°56'E	13:46:12	16:15:08	15:05:31	67.7%
East London	33°00'S	27°55'E	13:39:58	16:06:26	14:57:27	58.7%
Johannesburg	26°15'S	28°00'E	13:39:35	16:17:01	15:03:46	73.5%
Kimberley	28°43'S	24°46'E	13:31:59	16:09:14	14:55:32	65.3%
Port Elizabeth	33°58'S	25°40'E	13:35:15	16:01:33	14:52:22	55.2%
Pretoria	25°45'S	28°10'E	13:40:00	16:17:53	15:04:29	74.8%

5.3.3 The weather

In general, the meteorological conditions over South Africa in mid-winter are dominated by a strongly developed high-pressure system on the surface, echoed in the upper-air over the interior. This is accompanied by a regular succession of cold fronts sweeping the Western Cape and coastal areas up to Northern Kwa-Zulu Natal, often stretching far inland and causing partly cloudy to cloudy conditions in some places. In general, these conditions prevailed over South Africa at the time of the 2001 eclipse.

The weather events leading to the eclipse day on 21 June 2001 are now described in more detail, using daily 12:00 UT synoptic maps featured in Figures 5.3 to 5.6 (SAWB, 2001).

Starting three days before the eclipse day (viz., on 18 June 2001), a cold front passes over the southern interior causing partly cloudy and cold conditions in its wake (Figure 5.3). Over the interior, fine weather dominates well ahead of the cold front. From the far west, the Atlantic High ridges eastward. There is a reasonable chance to expect an upper-air trough accompanying the cold front sweeping the country.

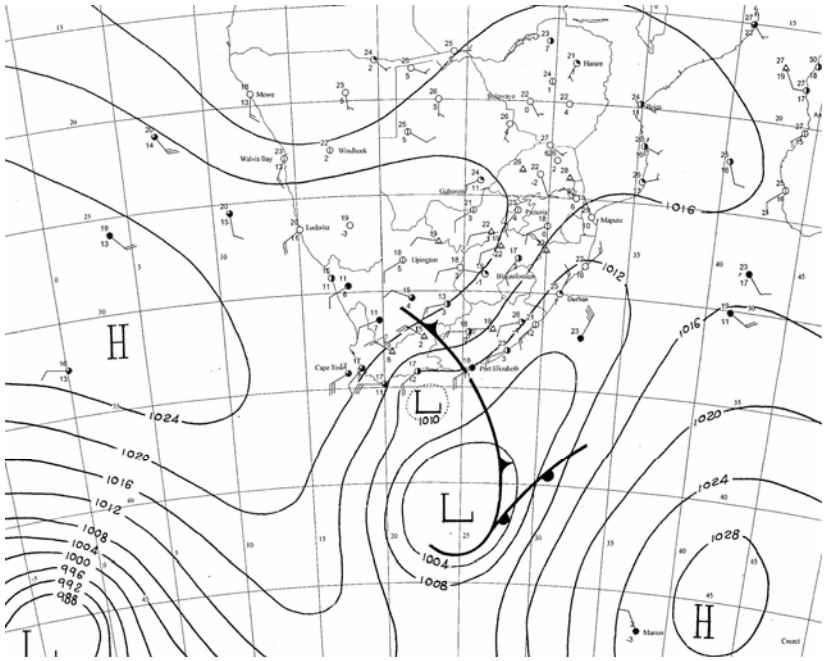

Figure 5.3 *Synoptic conditions at 12:00 UT on 18 June 2001 - three days before eclipse day (SAWB, 2001)*

The following day, 19 June 2001, the cold front had swept the eastern parts of the country, bringing partly cloudy and windy conditions in its wake. The Atlantic Ocean High ridging in behind it, causes rapid clearing from the west, with cold conditions and strong winds along the coast. (Figure 5.4.). The high-pressure system now extends over the country's interior and dominates the circulation, advecting cold air over the southern parts.

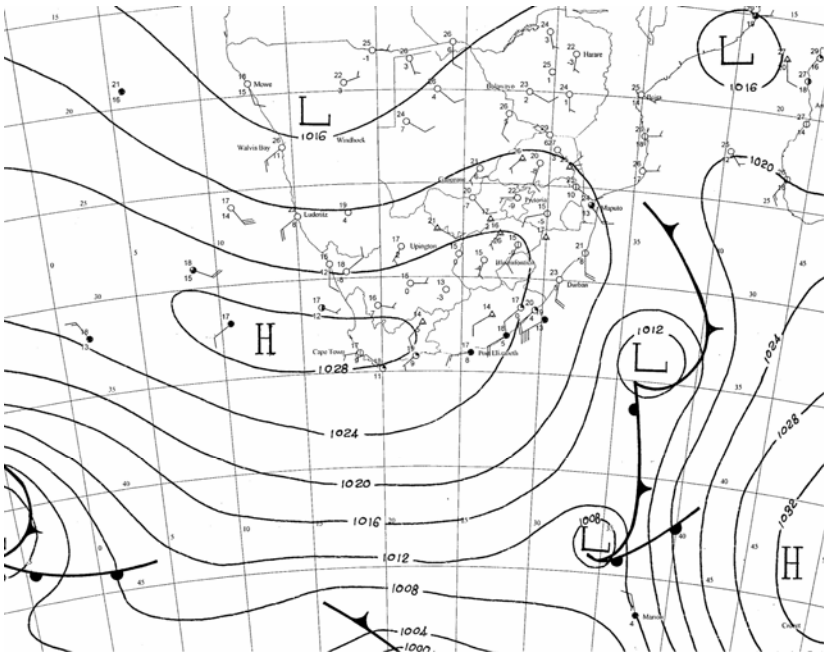

Figure 5.4 *Synoptic conditions at 12:00 UT on 19 June 2001 - two days before eclipse day (SAWB, 2001)*

The following day, 20 June 2001 (eclipse eve), the high-pressure system had established itself south-East of the continent (Figure 5.5). The advection of moist, cool air towards the eastern parts of the country lead to partly cloudy to cloudy and windy conditions along the coast of Kwa-Zulu Natal. The development of two small areas of low pressure (a twin-low pressure system) east of Durban, created a pressure gradient for strong onshore flow, aiding in the advection of moisture. Over the South African interior, conditions favoured the development of an upper-air ridge, causing subsidence and clear sky over most of the interior.

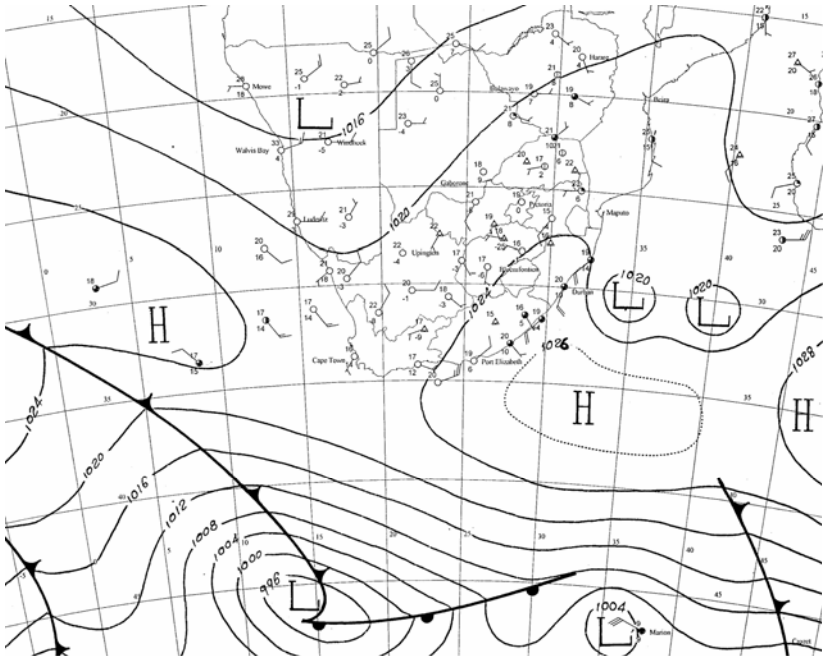

Figure 5.5 *Synoptic conditions at 12:00 UT on 20 June 2001 - one day before eclipse day (SAWB, 2001)*

On eclipse day, 21 June 2001, the circulation was dominated by a high-pressure system over the country's interior, centered where the borders of South Africa, Botswana and Zimbabwe meet (Figure 5.6). A cold front was situated to the far south and the Atlantic Ocean High, still deepening, advected warm air ahead of the front further west, pushing the front southwards and leading to only partly cloudy conditions along the southern coast.

A coastal low developed in the East London area, causing partly cloudy conditions in its wake. The twin low-pressure cells have migrated further northwards east of Maputo, whilst still maintaining a weak onshore flow, creating partly cloudy conditions along the northernmost parts of the South African eastern coastline.

It follows from Figure 5.6, that cloudless skies (good eclipse weather) were dominant over most of the country, except the southern coast and the eastern coastline. In particular, no clouds were present over the De Aar BSRN station.

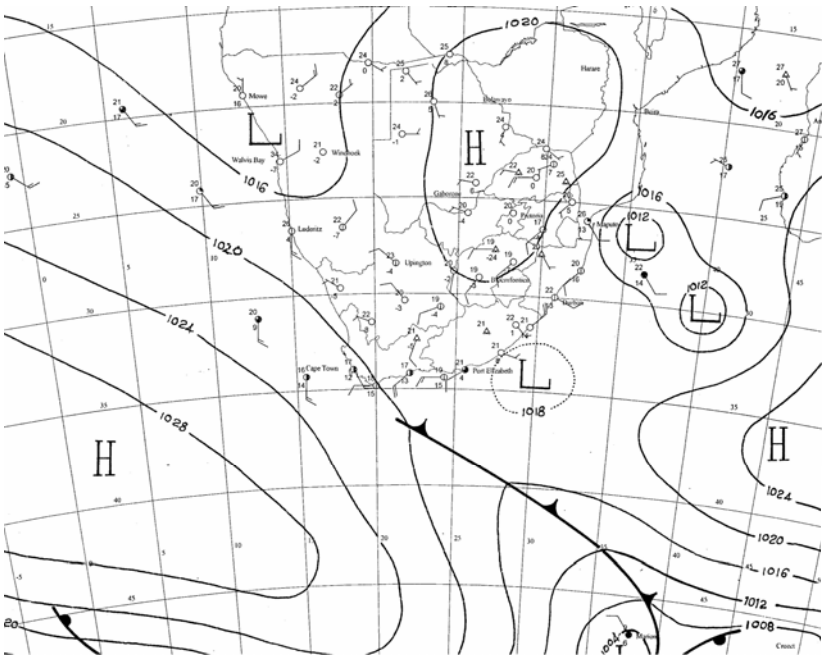

Figure 5.6 *Synoptic conditions at 12:00 UT on 21 June 2001 - eclipse day (SAWB, 2001)*

5.3.4 The BSRN measurements

The term “datapoint” refers to the standard one-minute average value as measured at BSRN stations. Consider Figure 5.7, showing a time-series of SW datapoints for eclipse day 2001.

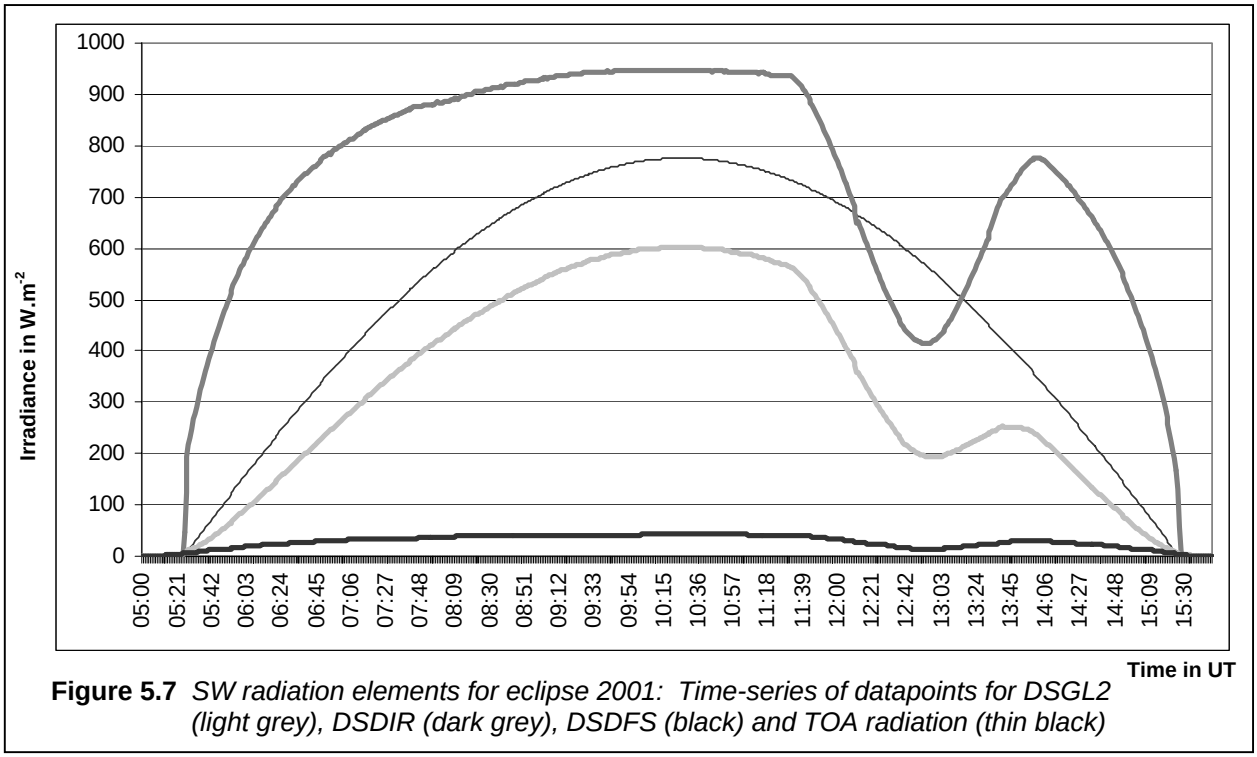

Figure 5.7 *SW radiation elements for eclipse 2001: Time-series of datapoints for DSGL2 (light grey), DSDIR (dark grey), DSDFS (black) and TOA radiation (thin black)*

Eclipse day (21 June) in 2001, was a clear sky day, resulting in smooth curves for all the SW components, hence showing the eclipse in a distinct and unique way. In Figure 5.7, DSDIR (direct), DSDFS (diffuse) and DSGL2 (global) radiation each show a smooth regular dip at the time of the partial eclipse (11:30 UT to 14:04 UT). The exception was the theoretically calculated TOA radiation.

One special remark about DSDFS: Under normal circumstances, when DSGL2 and DSDIR decrease, it is accompanied by and *increase* in DSDFS, usually due to the presence of clouds. In the presence of broken clouds or under overcast conditions, a distorted pattern is displayed, like Figure 4.19. Between datapoints, the DSDFS relation to the other two SW components usually holds, since the occulting (diffusing) objects are *inside* the atmosphere.

The smooth indentation in Figure 5.7 is uncharacteristic of clouds, and the fact that DSDFS *decreased* in synchronization with DSDIR and DSGL2 on this particular day, means that the object of occultation was *outside* the atmosphere, i.e., a celestial object such as the moon.

5.3.4.1 Radiation loss due to eclipse

From datapoints of 21 June 2001, the radiation loss as a result of the eclipse, is now estimated for all the SW components in Figure 5.7. Let R be the integrated radiation for a specific component, and R_0 the "ideal" integrated radiation if there was no eclipse. Hence the radiation loss due to the eclipse is the difference between R_0 and R.

R equals the area under each curve in Figure 5.7, and the area under a smooth curve is approximated by the sum of trapezium elements E_i :

$$R = \sum_{i=05:21}^{i=15:31} E_i \qquad (5.1)$$

Each E_i has width W = 1 minute and side heights I_i and I_{i+1}, where I = average incident radiation over the one-minute interval. Since, for a trapezium,

$$E_i = \frac{W}{2}(I_i + I_{i+1})$$

it follows from Equation 5.1 that $$R = \sum_{i=05:21}^{i=15:31} \frac{W}{2}(I_i + I_{i+1}) \quad (5.2)$$

Datapoints from the same day are used to estimate R_0, based upon the fact that the entire day was cloud-free. Under normal circumstances, the time-series for any SW radiation component, measured during a cloud-free day, is symmetric around the solar transit time. An estimation for R_0 is therefore twice the area under each curve in Figure 5.7 from sunrise (05:21 UT) to (10:26 UT), therefore twice the half-day excluding the eclipse. Hence:

$$R_0 = 2\sum_{i=05:21}^{i=10:26} E_i = 2\sum_{i=05:21}^{i=10:26} \frac{W}{2}(I_i + I_{i+1}) = \sum_{i=05:21}^{i=10:26} W(I_i + I_{i+1}) \quad (5.3)$$

Using Equations 5.2 and 5.3:

R_0(Global)	= 13653 kJ.m^{-2}	;	R(Global) = 12590 kJ.m^{-2}
R_0(Direct)	= 29429 kJ.m^{-2}	;	R(Direct) = 27186 kJ.m^{-2}
R_0(Diffuse)	= 1218 kJ.m^{-2}	;	R(Diffuse) = 1117 kJ.m^{-2}

Therefore, radiation loss due to the 2001 eclipse amounts to:

Global :	1063 kJ.m^{-2}	(7.78%).
Direct :	2243 kJ.m^{-2}	(7.62 %).
Diffuse:	101 kJ.m^{-2}	(8.34 %).

5.3.4.2 Focus on SW elements

In this Section, patterns for the following radiation datapoints for the 2001 eclipse are shown:

- BSRN one-minute standard deviations (OSD) for SW components.
- The DSGL2 : DSGL1 relationship.
- The normalized K-plots as used by NREL (1993)
- LWD radiation and individual terms of pyrgeometer Equation 3.4.

In each of Figures 5.8 to 5.10, the behaviour of a SW component, as well as the associated OSD for eclipse day, 20 June 2001, is displayed. The scale of the left Y-axis is associated

with the SW component in W.m^{-2}, while the scale of the right Y-axis is associated with the relevant OSD (dimensionless).

Figure 5.8 depicts DSDIR (direct irradiance) and associated OSD for eclipse day 2001.

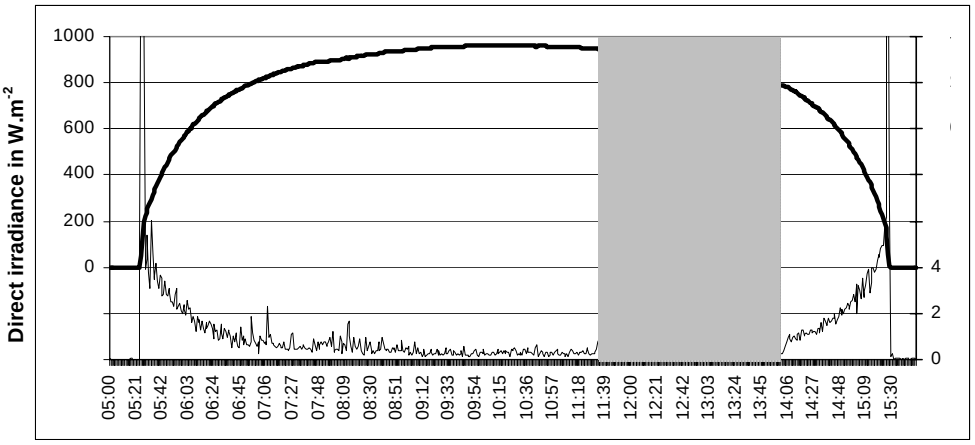

Figure 5.8 *DSDIR and the associated OSD. Eclipse time is shaded.*

Relatively low OSD values (roughly less than 1) outside the eclipse time and between one hour after sunrise and one hour before sunset, indicate just how clear the sky was during eclipse day. The value of OSD is a direct indication of the change in DSDIR from one minute to the next. For about the first hour after sunrise and the hour before sunset, OSD values are more than 1, indicating a rapid change in DSDIR from one minute to the next, which reaches a maximum when the sun is near the horizon. On the minute before sunrise, OSD is still zero, and in the first minute after sunrise, it is a high value (more than 10) since the appearance of the sun constitutes a big change in OSD. A similar argument holds for sunset. At solar noon (10:26 UT), OSD is expected to reach a minimum value.

During the day, outside the eclipse time, small variations in OSD from one minute to the next, occur on almost a continuous basis, in the form of “background noise”. The background noise becomes markedly less during the eclipse, indicating that the variation from one minute to the next, as a result of the eclipse, supercedes the background noise, which one can assume to be still present during the eclipse. An interesting zero-point in OSD is reached during the middle of the eclipse (12:52 UT). The zero point is surrounded by two local maxima.

Figure 5.9 depicts DSGL2 (global irradiance) and associated OSD. Figure 5.9 shows similarities with Figure 5.8: The same OSD background noise, but slightly larger in

magnitude, but also suppressed during the eclipse, for the same reason as DSDIR. The maximum daily DSGL2 is less than DSDIR, and the DSGL2 curve is also "flatter".

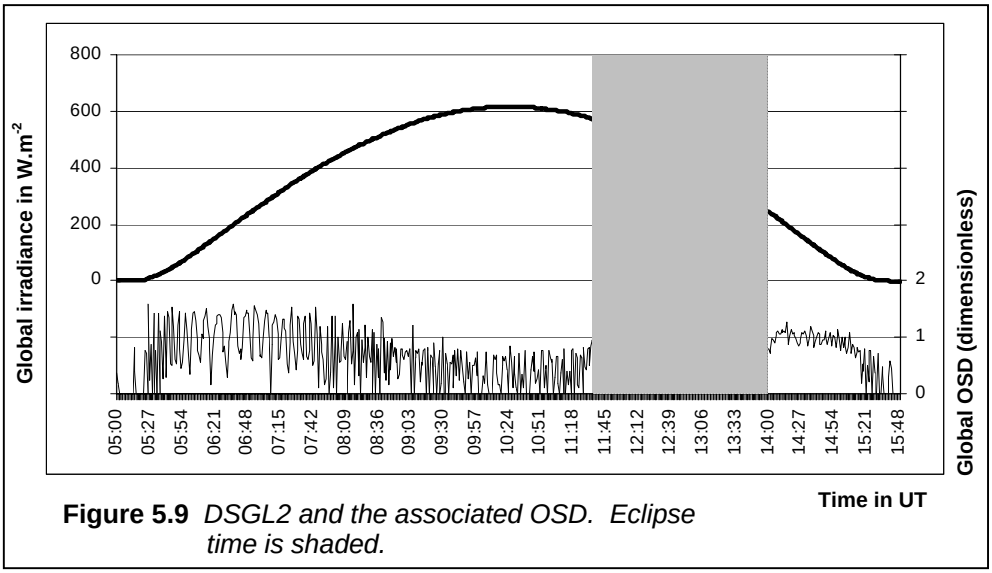

Figure 5.9 *DSGL2 and the associated OSD. Eclipse time is shaded.*

Figure 5.10 depicts DSDFS (diffuse irradiance) and associated OSD.

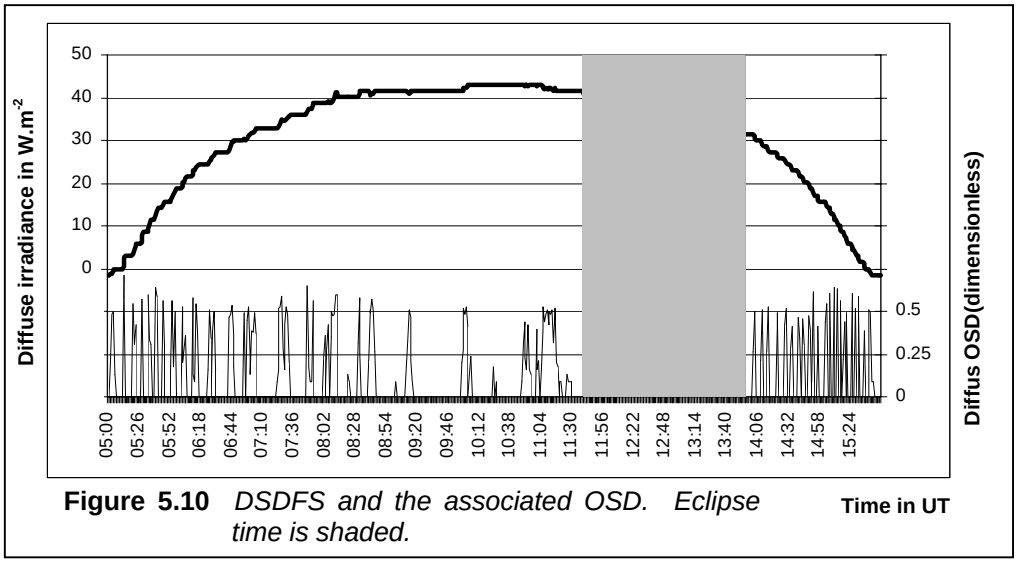

Figure 5.10 *DSDFS and the associated OSD. Eclipse time is shaded.*

In Figure 5.10, the magnitude of the numbers is less than in Figure 5.8 or Figure 5.9. Therefore, small amounts of background noise will feature as relatively larger numbers. The presence of the solar eclipse is clearly marked in the DSDFS time-series, and a small variation of OSD during the middle of the eclipse. Keep in mind that diffuse radiation is in general a more conservative parameter as far as variations due to changing atmospheric conditions are concerned. The attention is now focused on DSGL1 (global irradiance calculated using DSDIR and DSDFS) and DSGL2 (global irradiance directly measured using an unshaded pyranometer).

For any solar zenith angle Z at time instant t, DSGL1 is defined (Gilgen *et al.*, 1995) as:

$$DSGL1(t) = DSDFS(t) + DSDIR(t).\cos Z \qquad (5.4)$$

Figure 5.11 shows a time-series of the absolute difference DSGL2–DSGL1 and the ratio DSGL2/DSGL1 for eclipse day, 21 June 2001. Eclipse time is shaded.

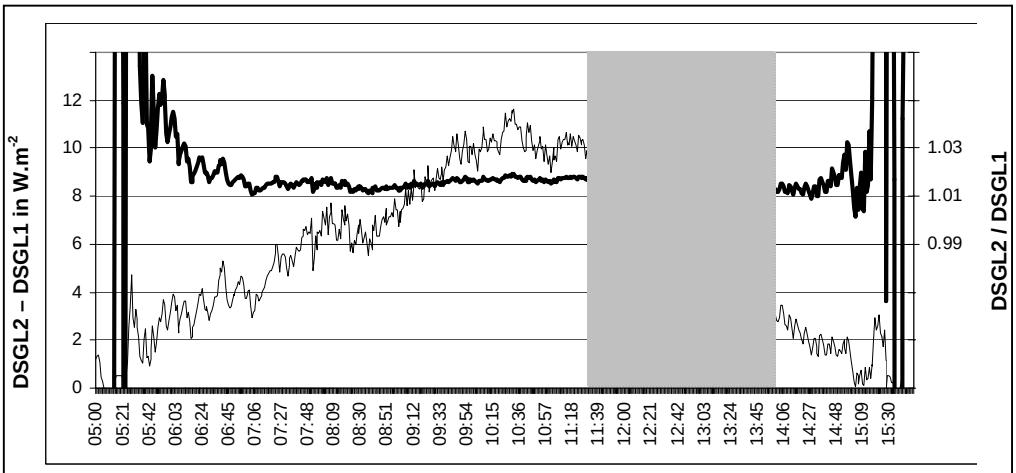

Figure 5.11 *Time-series of DSGL2–DSGL1 (thin line) and DSGL2/DSGL1 (thick line). Eclipse time is shaded.*

From Figure 5.11 it is evident that DSGL2/DSGL1 is conservative with respect to the solar eclipse, since the eclipse (shaded area) has no visible influence on its time-series. To a lesser extent this is also true for (DSGL2-DSGL1). Disruptions in these specific time-series are the result of "shocks" where the different instruments measuring DSGL2, DSDIR and DSDFS recover at different rates to a passing cloud or the sun rising/setting. Evidence of this behaviour can be seen in Figure 5.11 roughly at 05:20 UT and 15:30 UT. During the eclipse, none of these shocks are visible. An explanation is, that the transition in intensity during the eclipse from one minute to the next was smooth enough, so that the instruments under consideration could adjust accordingly.

Using TOA radiation as normalization factor, definitions for K-plots (NREL, 1993) can be defined for the SW components, per datapoint, at time instant t and solar zenith angle Z:

- K_n = DSDIR(t) * cos$Z$ / TOA(t)
- K_t = DSGL2(t) / TOA(t)
- K_d = DSDFS(t) / TOA(t)

The time-series for K_n , K_t and K_d as well as $K_t - (K_n + K_d)$, are depicted for 21 June 2001 in Figure 5.12.

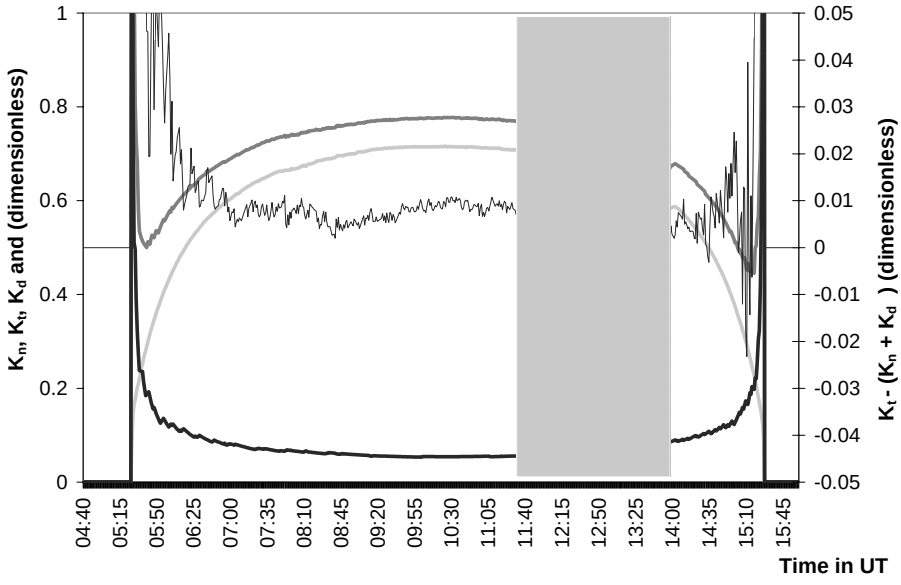

Figure 5.12 *Time-series for K_t (light grey), K_n (dark grey), K_d (thick black), and $K_t - (K_n + K_d)$. Eclipse time is shaded.*

Each of K_n , K_t and K_d shows the eclipse presence in a clear indentation, the latter less distinct, . The slight "noise" in $(K_t - (K_n + K_d))$ is insignificant, keeping in mind that the scale for $(K_t - (K_n + K_d))$ is ten times that of the other parameters in Figure 5.12.

Another NREL analysis method is a scatter diagram of K_n vs K_t, for Z < 80°, (Figure 5.13):

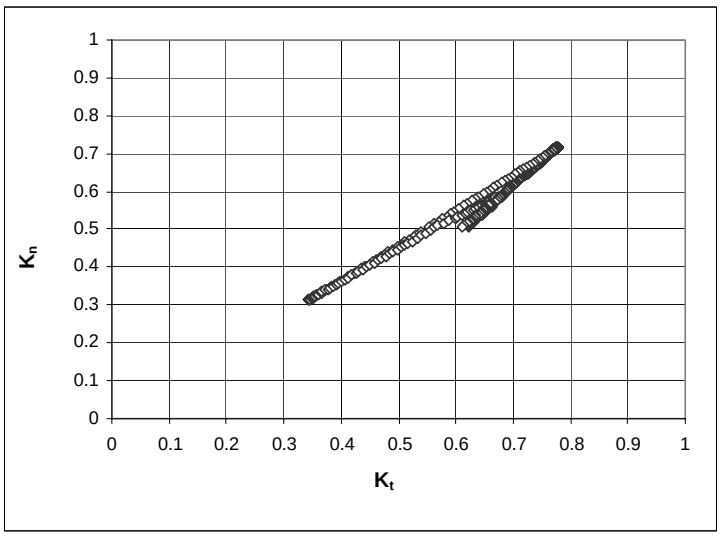

Figure 5.13 *Scatter diagram of K_n versus K_t for 21 June 2001*

No major deviations from a straight line are observed in Figure 5.13, which leads to the conclusion that K_n, and K_t are conservative for this data representation with respect to the eclipse on a clear day. The slight "hook" between K_t = 0.6 ; K_n,= 0.5 and K_t = 0.78 ; K_n,= 0.72 indicates the presence of the solar eclipse. See also Figure 5.32.

5.3.4.3 Focus on LW elements

In the pyrgeometer Equation 3.4, the significance of each of the three terms, as well as LWD, were discussed in Section 3.1.3.1. Figure 5.14 represents time-series of the three terms of Equation 3.4, as well as LWD.

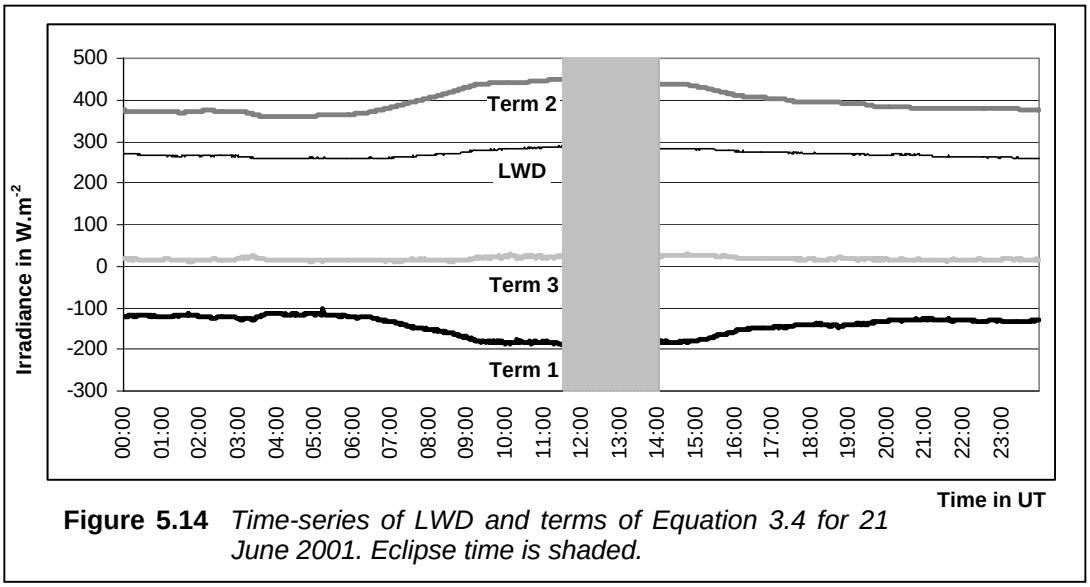

Figure 5.14 *Time-series of LWD and terms of Equation 3.4 for 21 June 2001. Eclipse time is shaded.*

Figure 5.14 resembles Figure 3.5 (a clear sky winter day). Term 2 is mirrored by Term 1 to a large extent and Term 3 is relatively small. This means that there is a small diurnal variation in LWD, in line with a clear sky winter day. All four time-series during the eclipse (shaded area in Figure 5.14) are not noticeably different from the areas outside the eclipse, therefore the eclipse of 21 June 2001 had no major effect on LWD or any of its terms. In Figure 5.15, only the LWD data for eclipse day was plotted, using a different scale. Eclipse time is shaded.

Note in Figure 5.15, that the LWD only increases about 1 hour after sunrise. The same delay is observed in the maximum LWD only reached about 1 hour after the maximum solar input had been reached (solar noon). The same effect is not so explicit after sunset. It should be kept in mind, that no clouds were present on that day, therefore only the effect of

the atmosphere is portrayed. The diurnal maximum LWD is 298 W.m^{-2} and the minimum is 251 W.m^{-2}. The eclipse (shaded area) however, does not seem to make a noticeable impact on LWD.

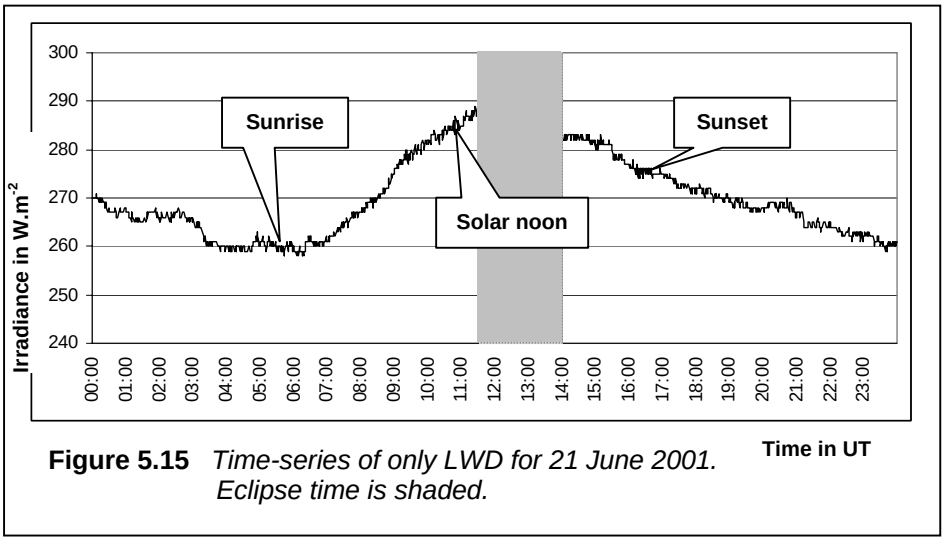

Figure 5.15 *Time-series of only LWD for 21 June 2001. Eclipse time is shaded.*

For a closer zoom on the behaviour of LWD during the eclipse, consider Figure 5.16.

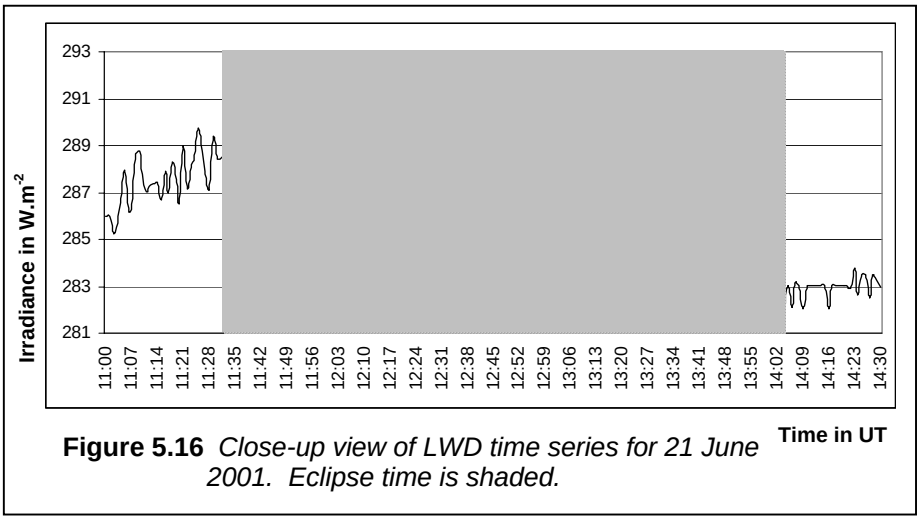

Figure 5.16 *Close-up view of LWD time series for 21 June 2001. Eclipse time is shaded.*

Keeping the delay of about 1 hour in mind, as observed in Figure 5.15, no noticeable changes in LWD as a result of the eclipse, are observed in Figure 5.16.

5.3.4.4 Non-radiation measurements

The 5-minute meteorological data for the eclipse day was extracted from the co-located AWS. Figure 5.17 depicts a time-series of the surface (Stevenson Screen) temperature and relative humidity, with eclipse time shaded. Keep in mind that relative humidity is dependent upon temperature, explaining the apparent mirror-images. If one inspects the eclipse period,

a steady drop in temperature of about 3°C, followed by a small rise of 1°C, is observed. This trend is inverted in the time-series of the relative humidity.

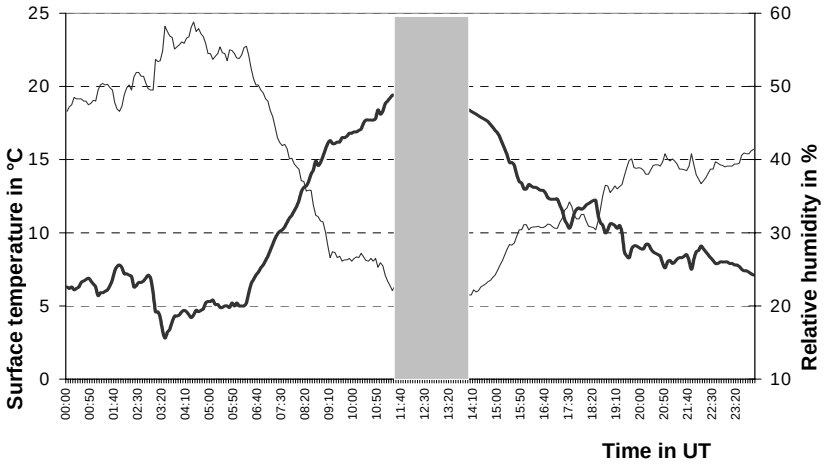

Figure 5.17 *Time-series of surface temperature (thick line) and relative humidity (thin line) for eclipse 2001. Eclipse time is shaded.*

In Figure 5.18, time-series of the wind speed and wind direction are presented, with eclipse time being shaded.

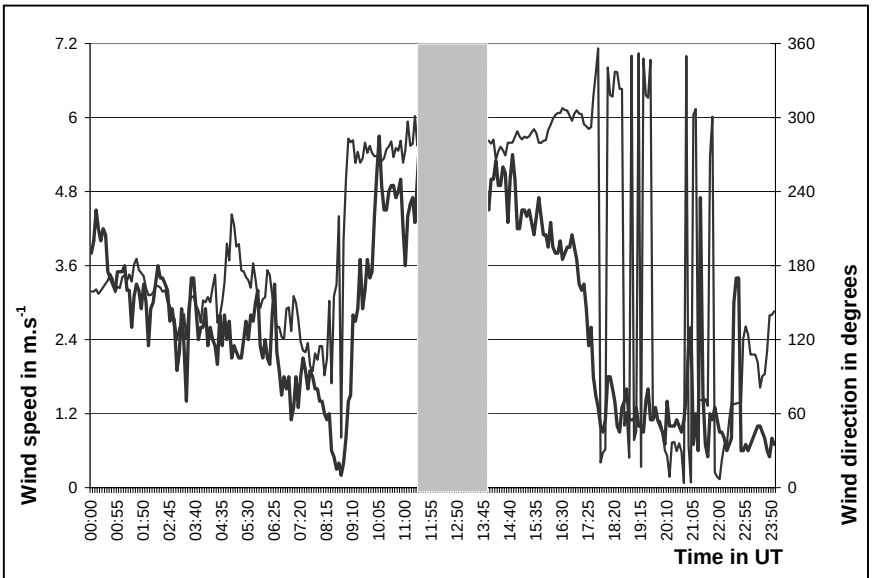

Figure 5.18 *Time-series of wind speed (think line) and wind direction (thin line) for elipse 2001. Eclipse time is shaded.*

The wind speed increased strongly in the mid-morning (at around 09:00 UT) and reached a maximum at about 12:00 UT. By this time the eclipse had already started. A sharp decrease in wind speed is observed for almost the rest of the eclipse, recovering after the end of the eclipse, and returning to calm at about 18:00 UT. During the eclipse, the wind direction remained roughly constant, viz., 270° (West).

5.4 ECLIPSE OF 4 DECEMBER 2002

5.4.1 General description

The path of totality for this total solar eclipse is illustrated in a global context in Figure 5.19 and in more detail in Figure 5.20, using an even closer up view in Figure 5.21.

In Figure 5.19, the path of totality is represented by the thick central line starting off the Angolan coast, crossing Southern Africa, curving upwards as it crosses the Southern Indian Ocean, entering the Australian Bight and ending in the Outback. The thinner lines parallel to this line respectively represent the 80%, 60%, 40%, 20% and 0% phases, respectively, of the partial eclipse. The dashed line orthogonal to the path of totality, stretching from a point in the central Indian Ocean directly south of India, towards Antarctica, represents the peak line. The intersection between this line and the path of totality west of Angola, is the eclipse peak at 39°27' S, 59°33' E, where the path of totality had its maximum width (90 km). For an observer at that point, the eclipse occurred at 07:31:11 UT, 102.5% of the solar disk was obscured, and totality would last 2'08".

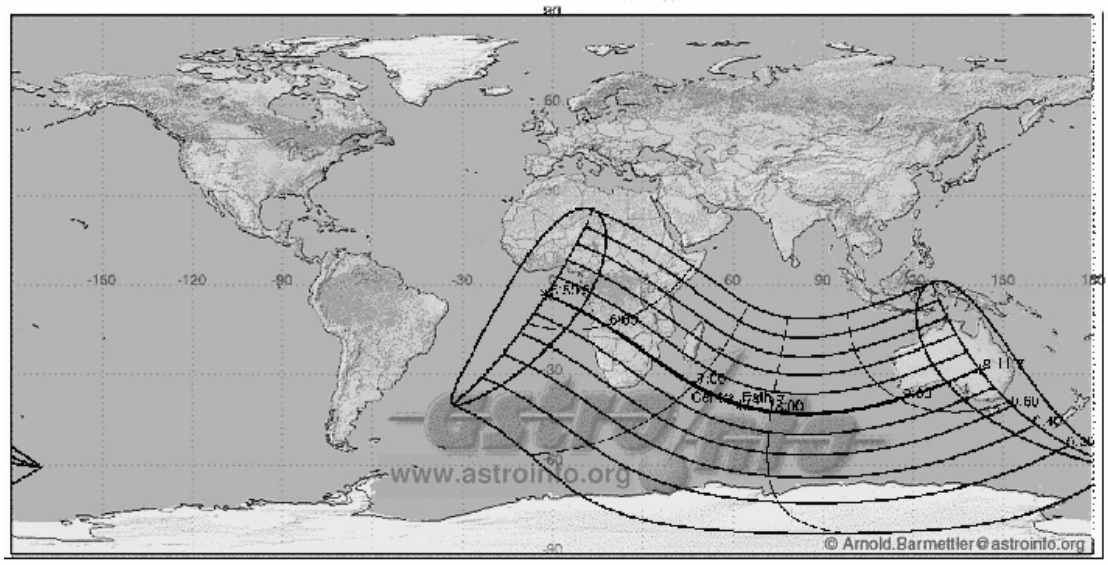

Figure 5.19 *Global orthographic projection of solar eclipse, 4 December 2002. Map by Arnold Barmettler at Astro-Info (www.astro-info.org)*

Note that totality path width, central duration and solar disk obscuration are significantly smaller than during the 2001 eclipse. Since South Africa is located to the west of the eclipse peak this time, the eclipse 2002 was observed in the waxing phase. The 2002 path of totality also intersected a 40 km narrow strip on the Angolan coast (Figure 5.20), where the

2001 eclipse crossed into Africa. This means, that totality was experienced here twice in less than a year and a half.

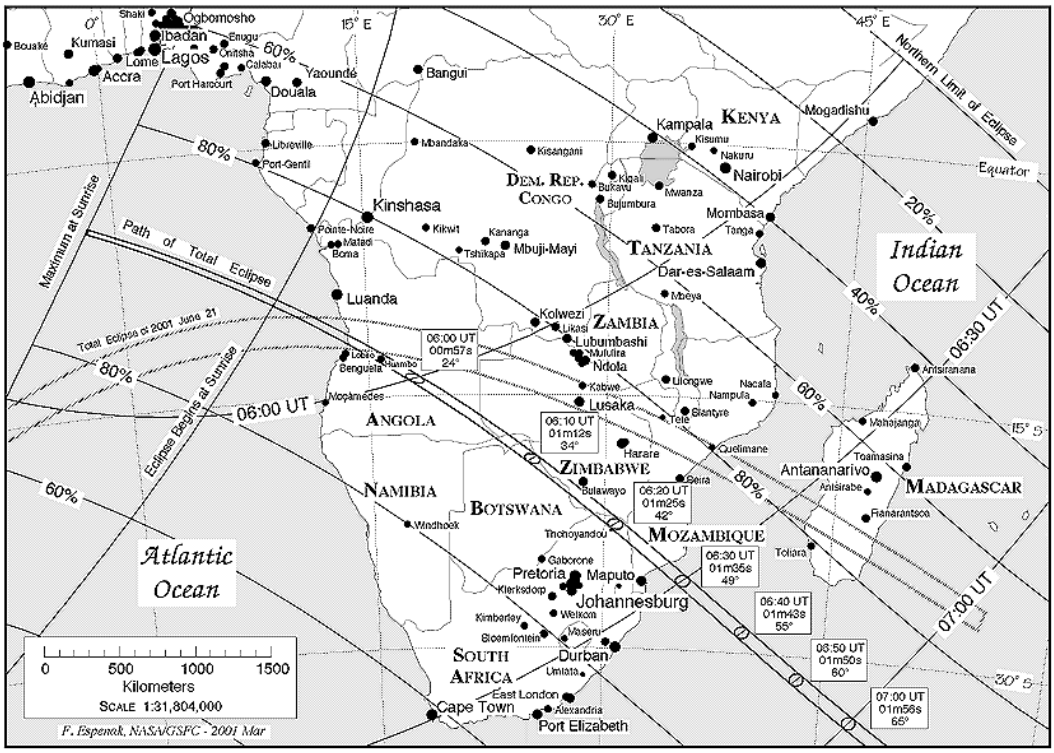

Figure 5.20 *Close-up view of the 2002 eclipse path through Africa, showing details of the partial phase. For reference, the totality path for 2001 is also shown. Map after Espenak and Anderson (2001). Times in UT.*

In Southern Africa (Figure 5.20), the path of totality crosses Southern Angola, the Caprivi Strip of Namibia, and runs almost along the Zimbabwe-Botswana border. It clips the northernmost part of the Limpopo Province of South Africa, before crossing southern Mozambique. Messina, South Africa, was the most populated point under the totality path.

5.4.2 Eclipse in South Africa

As mentioned before, this is the first time since 1 October 1940, that the path of totality of an eclipse covered South African soil. Phase magnitudes ranged between 60 % at Cape Town in the extreme south-west, and up to more than 100 % at Messina.

The close-up view in Figure 5.21 shows the path of totality, as well as the partial 80% and 60% phase lines. All times in UT.

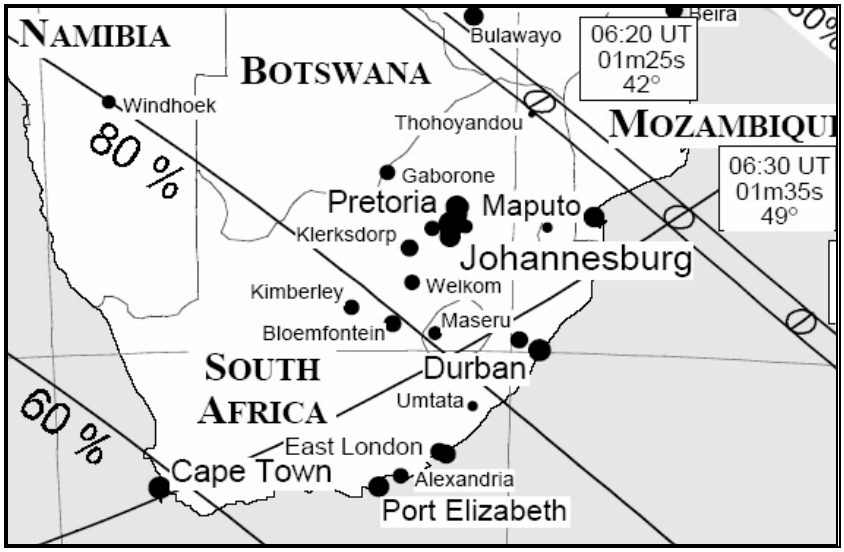

Figure 5.21 *Close-up view of totality path and partial phases for South Africa. Map after Espenak and Anderson (2001) and cropped.*

Table 5.4 shows local circumstances for a few major centra during the 2002 eclipse (Espenak and Anderson, 2001).

Table 5.4 *Local circumstances for major South African centra during the 2002 eclipse.*

Location	Latitude	Longitude	First contact	Last contact	Max eclipse	Magni-tude
Bloemfontein	29°12'S	026°07'E	07:22:30	09:39:10	08:26:53	79.3%
Cape Town	33°55'S	018°22'E	07:32:11	09:32:33	08:29:28	58.7%
Durban	29°55'S	030°56'E	07:24:42	09:48:26	08:32:18	85.1%
East London	33°00'S	027°55'E	07:29:59	09:47:03	08:34:46	74.1%
Johannesburg	26°15'S	028°00'E	07:17:35	09:38:10	08:23:33	88.5%
Kimberley	28°43'S	024°46'E	07:21:32	09:36:20	08:25:03	78.3%
Port Elizabeth	33°58'S	025°40'E	07:31:43	09:44:17	08:34:31	68.8%
Pretoria	25°45'S	028°10'E	07:16:46	09:37:41	08:22:51	89.9%

5.4.3 The weather

Since the eclipse occurred in mid-summer, the typical summer synoptic weather pattern for South Africa can be expected, which comprises surface and upper-air troughs over the interior joining the Inter-tropical Convergence Zone (ITCZ). In such a situation, tropical moist air is circulated over the interior, causing thundershowers associated with the uplift by virtue

of upper-air troughs and heat convection. Around the coast, high-pressure systems advect cool maritime air, adding orographic precipitation on the wind-side of high-lying areas. The presence of quasi-stationary high-pressure systems, one to the west (Atlantic Ocean) and another to the east (Indian Ocean) causes frontal systems to pass well south (more than 40° South) so that cold fronts do not frequently sweep the country in summer time.

The weather leading to eclipse day is described in terms of a series of 12:00 UT surface synoptic maps (SAWS, 2002).

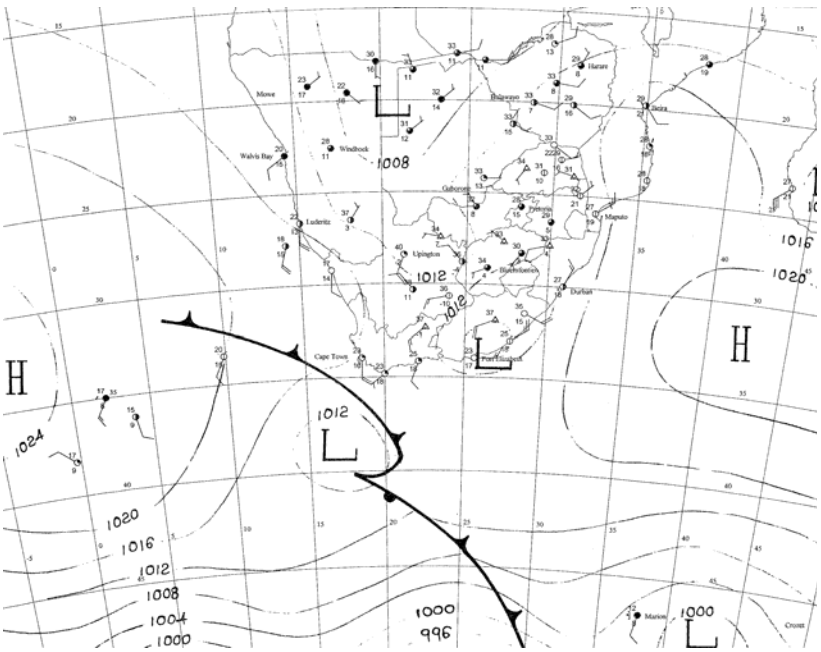

Figure 5.22 *Synoptic conditions at 12:00 UT on 1 December 2002 - three days before eclipse day (SAWS, 2002)*

On 1 December 2002 (Figure 5.22), three days prior to eclipse day, a surface trough is present over the western interior, feeding moist tropical air southwards, resulting in the development of isolated thundershowers over the provinces of North-West, Northern Free State, Gauteng and Mpumalanga. A cold front approaches the south-western Cape. Very hot conditions prevailed in the northern parts of the North Cape (Upington measuring 40°C).

Two days before eclipse day, 2 December 2002, (Figure 5.23), the interior surface trough was well-developed. The influx of moist, tropical air to the east of the trough-axis, brought partly cloudy to cloudy conditions with scattered thundershowers over the Northern and Eastern Cape, as well as isolated thundershowers over the North-West and in places over the Free State, Gauteng, Kwa-Zulu Natal and the Western Cape in lieu of what can be a closed separated cell of low pressure over the Karoo. Over the central interior, the conditions are ideal for the presence of an upper-air trough. The cold front passed to the far

south in the presence of the strong quasi-stationary high-pressure systems respectively in the Atlantic Ocean and the Indian Ocean, respectively.

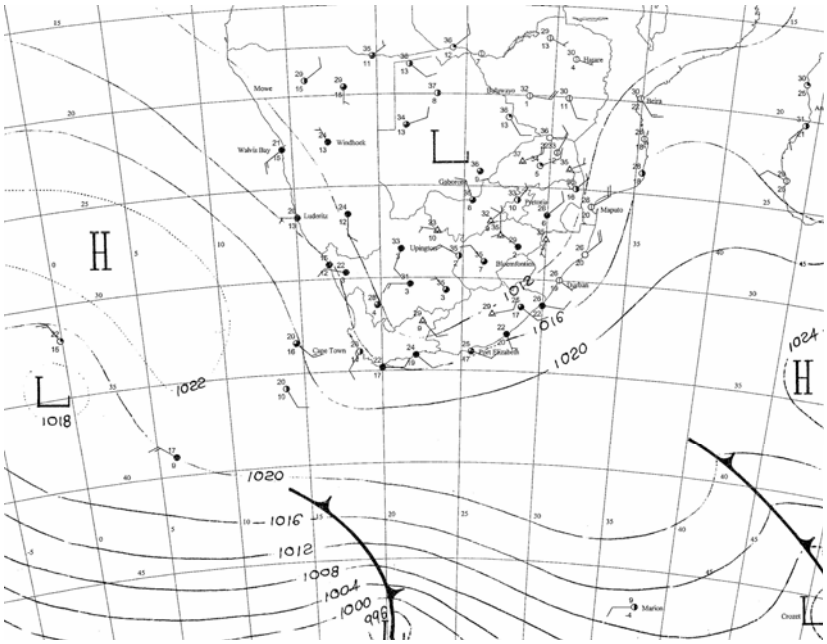

Figure 5.23 *Synoptic conditions at 12:00 UT on 2 December 2002 - two days before eclipse day (SAWS, 2002)*

On the following day, 3 December 2002, eclipse eve (Figure 5.24), the interior surface trough was still present and deepening, with an upper-air trough to the west of the surface trough.

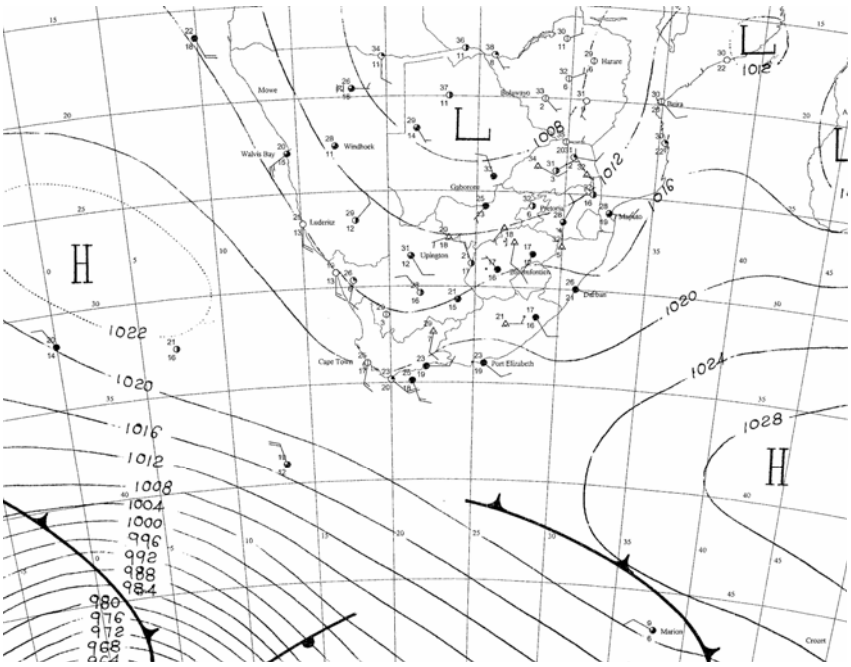

Figure 5.24 *Synoptic conditions at 12:00 UT on 3 December 2002 – one day before eclipse day (SAWS, 2002)*

The advected tropical air continued to bring widespread scattered thundershowers to the east of the trough-axis (parts of the Free State, North West, Eastern and Northern Cape and Kwa-Zulu Natal), including isolated thundershowers over Mpumalanga (SAWS, 2002).

On eclipse day, 4 December 2002, the meteorological scene was dominated by the interior surface trough, still deepening (Figure 5.25). Along the perimeter of the Indian Ocean High, a well- developed circulation was established, advecting moist air towards the eastern half of the country, aided by an influx of maritime air from the Mozambiquean channel. This caused overcast to partly cloudy conditions extending as far south as the central Free State and Lesotho. This was also accompanied by light rain in places, and rainfall totals of 1 to 3 mm were reported in those areas (SAWS, 2002).

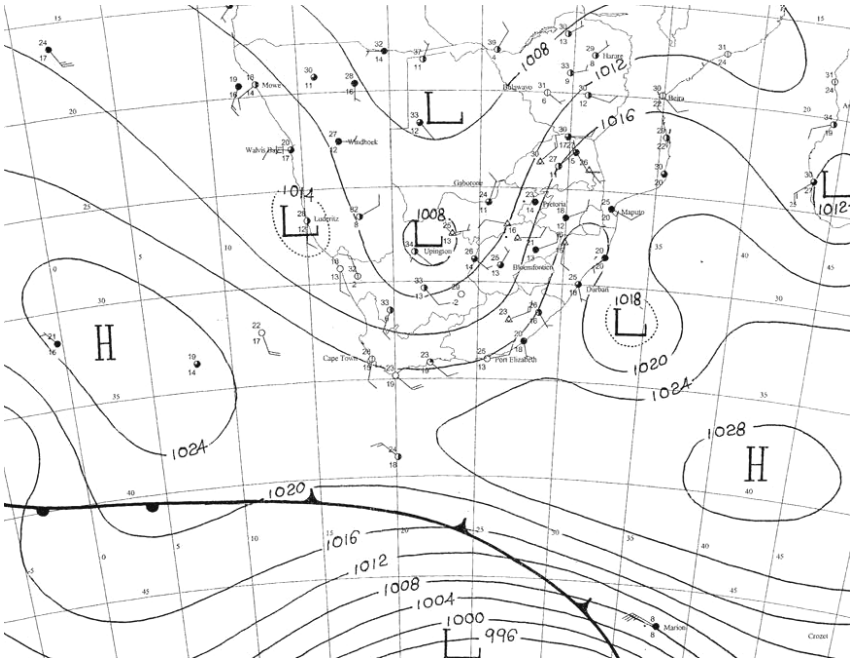

Figure 5.25 *Synoptic conditions at 12:00 UT on 04 December 2002 – eclipse day (SAWS, 2002)*

However, a well- defined low pressure system south-east of Durban, caused the axis of the surface and upper-air trough over the interior of the country to bend south-eastwards. This shifted the overcast to partly cloudy conditions eastwards, allowing the sky southwest of Bloemfontein to clear. De Aar BSRN station was in this region and hence experienced perfectly clear skies for the entire day, just like during the 2001 eclipse.

5.4.4 The BSRN measurements

Similar to the 2001 eclipse, a pristine set of SW measurements could again be performed at De Aar, by virtue of a cloud-free day. Figure 5.26 features the SW components together with TOA radiation, for eclipse day, 4 December 2002.

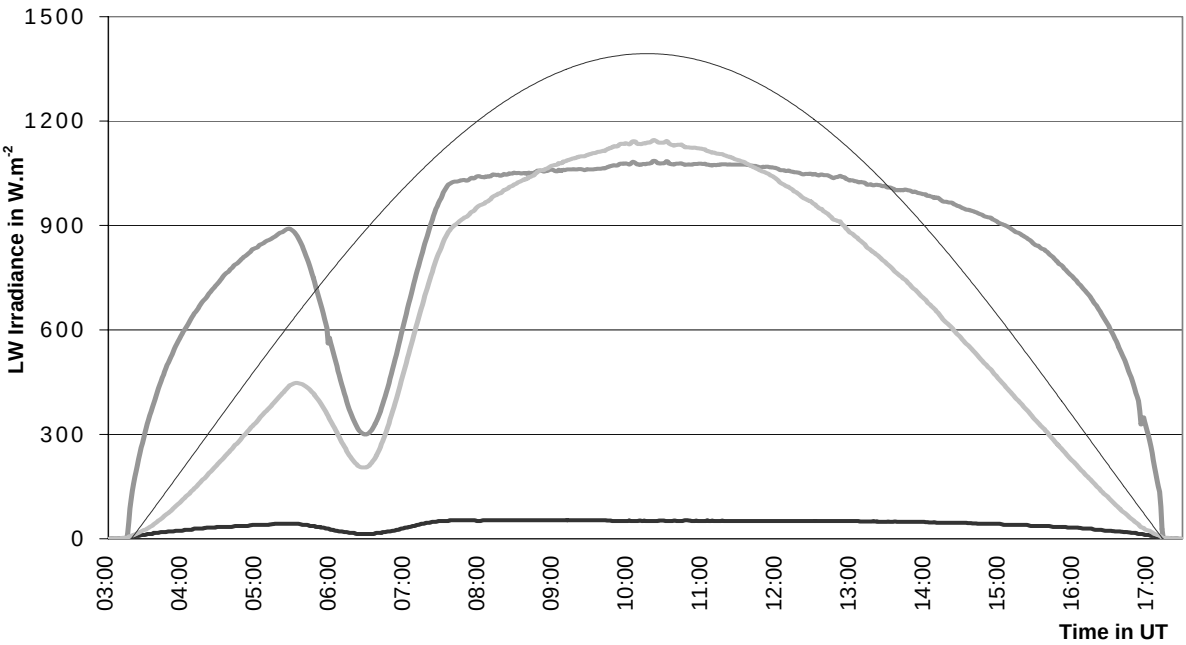

Figure 5.26 *SW radiation elements for eclipse 2002: Time-series of datapoints for DSGL2 (light grey), DSDIR (dark grey), DSDFS (black) and TOA radiation (thin black line)*

From Figure 5.26 it is clear, that the effect of the eclipse, and only the eclipse, appears in the time-series of DSDIR and DSGL2. The DSDFS shows the clear effect of an extraterrestrial object (moon) occulting the sun since an object in the atmosphere would have increased DSDFS and decreased the DSDIR.

5.4.4.1 Radiation loss due to eclipse

The amount of solar radiation loss on 4 December 2002 is calculated using the basic forms of Equations 5.2 and 5.3, adapted for sunrise (03:14 UT), solar transit (10:14 UT) and sunset (17:15 UT).

$$R = \sum_{i=03:14}^{i=17:15} E_i \qquad (5.5)$$

$$R_0 = \sum_{i=10:14}^{i=17:14} W(I_i + I_{i+1}) \qquad (5.6)$$

Using Equations 5.5 and 5.6 with datapoints for 4 December 2002:

R_0(Global) = 32537 kJ.m^{-2} ; R(Global) = 30513 kJ.m^{-2}

R_0(Direct) = 43292 kJ.m^{-2} ; R(Direct) = 40391 kJ.m^{-2}

R_0(Diffuse) = 2024 kJ.m^{-2} ; R(Diffuse) = 2121 kJ.m^{-2}

Therefore, radiation loss due to the 2002 eclipse amounts to:

Global : 2024 kJ.m^{-2} (6.22%)
Direct : 2901 kJ.m^{-2} (6.70%)
Diffuse : 97 kJ.m^{-2} (4.56%)

The radiation losses of the 2001 and 2002 eclipses are now compared in Table 5.5. Although solar disk obscuration was more in 2002 (73.1% in 2002 versus 60.7% in 2001), the day was also longer (14 hours and 1 minute in 2002 versus 10 hours and 10 minutes in 2001). Therefore, although the actual radiation loss in 2002 is more in absolute terms in 2002, it is smaller in relative terms as a result of a longer day. Global and direct radiation loss percentages are comparable for both eclipses, unlike the diffuse, which is considerably less in absolute terms.

Table 5.5 *Comparison of radiation losses for the two eclipses*

Eclipse	2001		2002	
	kJ.m^{-2}	%	kJ.m^{-2}	%
Global	1063	7.78	2024	6.22
Direct	2243	7.62	2901	6.70
Diffuse	101	8.34	97	4.56

5.4.4.2 Focus on SW elements

Datapoints of individual SW elements are now analyzed together with the corresponding OSD for eclipse day, 4 December 2002.

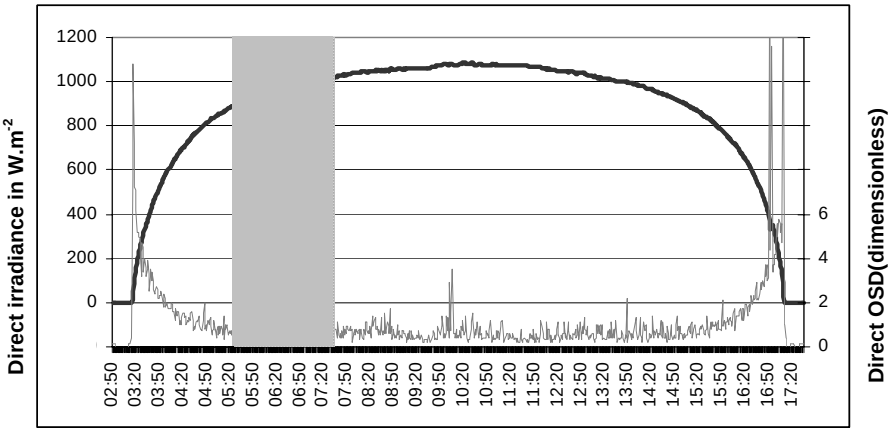

Figure 5.27 *DSDIR and the associated OSD. Eclipse time is shaded.*

The corresponding analysis of Figure 5.27 is shown in Figure 5.8 for the 2001 eclipse. The same level of background noise in OSD is experienced, except for a slight disturbance at about 10:10 UT. Put in context of the OSD values during the eclipse, it is relatively small and one can assume, that the same degree of sky clearness existed as during the 2001 eclipse.

The OSD values during the eclipse resemble the 2001 eclipse (Figure 5.8) with a zero point in the middle of the eclipse at 06:27 UT, surrounded by two local maxima, denoting a sharp change in DSDIR superceding the background noise which one can assume to be present. The same OSD anomalies for DSDIR during sunrise and sunset are also present during the 2002 eclipse. Figure 5.28 depicts DSGL2 for the 2002 eclipse together with the associated OSD.

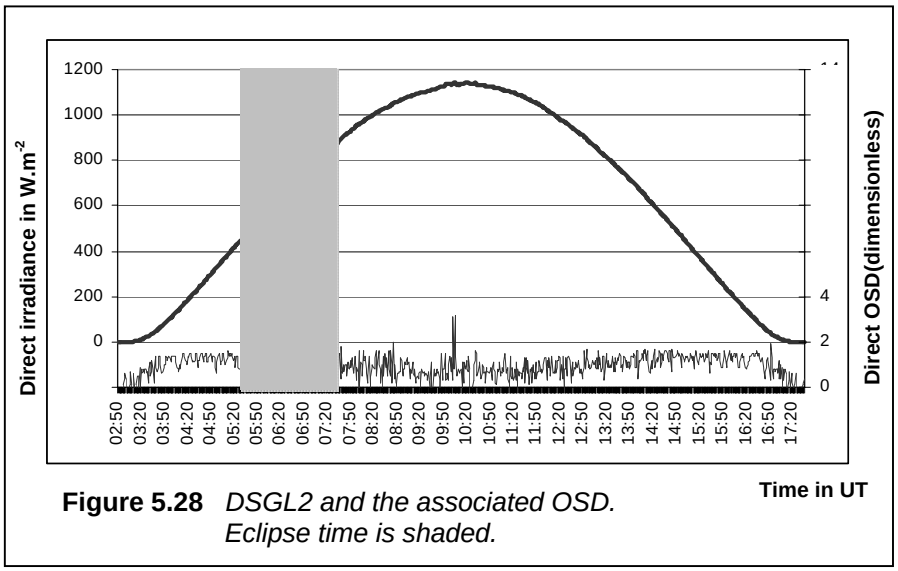

Figure 5.28 *DSGL2 and the associated OSD. Eclipse time is shaded.*

Figure 5.28 resembles Figure 5.10 (the corresponding graph of eclipse 2001). A distinct disturbance in OSD occurs at about 10:10 UT, but otherwise the level of background noise is comparable to that of the 2001 eclipse. During the eclipse, a zero-level OSD is experienced in the middle of the eclipse (06:28 UT), surrounded by two local maxima, the latter being larger in magnitude than the former, since the eclipse occurs as the sun is rising, and the change from one minute to the next is more significant when the sun is further from the horizon.

Figure 5.29 depicts DSDFS and the associated OSD. Eclipse time is shaded. The corresponding graph for eclipse 2001 is Figure 5.10, which also resembles Figure 5.29 to a large extent. Although the background noise in OSD is larger for the 2002 eclipse than the 2001 eclipse, the same distinct lower OSD values are present in the middle of the eclipse, surrounded by larger numbers for OSD.

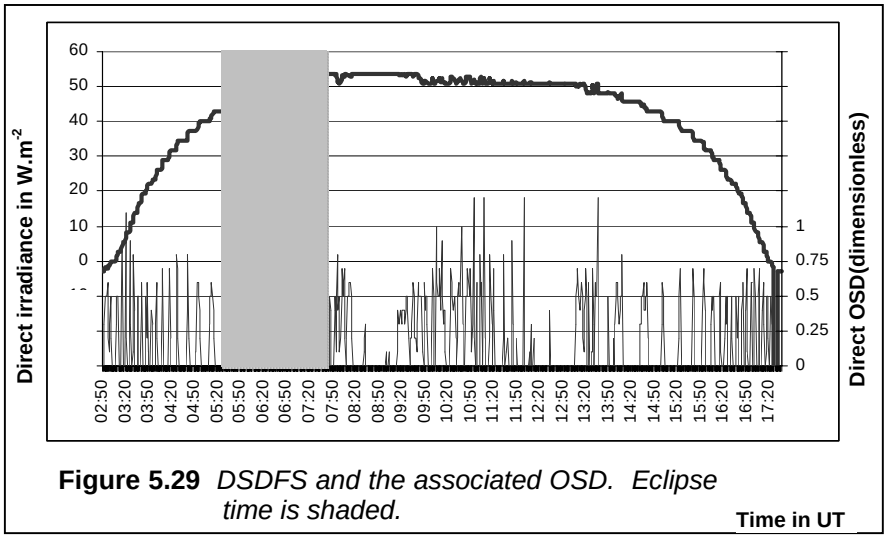

Figure 5.29 *DSDFS and the associated OSD. Eclipse time is shaded.*

In summary, the SW components and associated OSD values show similar features between the 2001 and 2002 eclipses. The background noise values of OSD are similar, which leads to the conclusion that the sky was equally clear on both days.

Next, the focus is placed on the relationship between DSGL1 and DSGL2. Figure 5.30 is a time-series of the ratio DSGL2 / DSGL1 as well as the absolute difference DSGL2 - DSGL1.

The graph corresponding with Figure 5.30 for the eclipse 2001 is Figure 5.11. The comparison shows that the relationship between DSGL2 and DSGL1 is very conservative with respect to the solar eclipse. In Figure 5.30, a clear disruption of DSGL2/DSGL1 can be

observed during eclipse 2002, which is not present outside the eclipse. An indentation in (DSGL2-DSGL1) is also present during the eclipse.

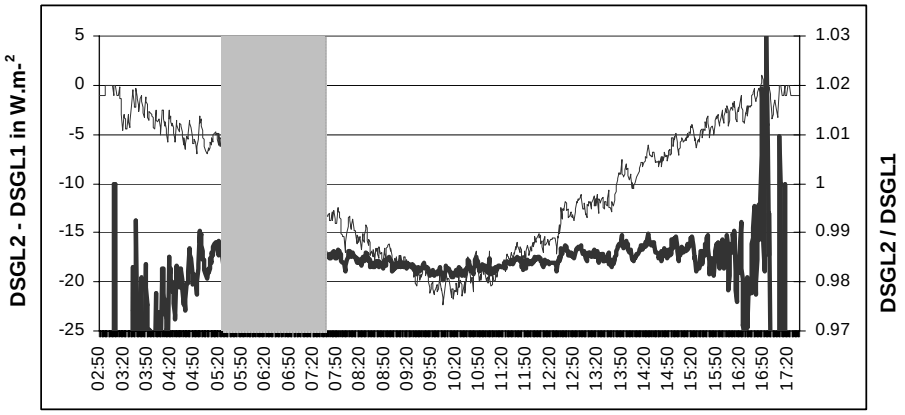

Figure 5.30 *Time-series of DSGL1 - DSGL2 (thin line) and DSGL2/DSGL1 (thick line). Eclipse time is shaded.*

K-plots are presented in Figures 5.31 and 5.32, similar to Figures 5.12 and 5.13 for the 2001 eclipse.

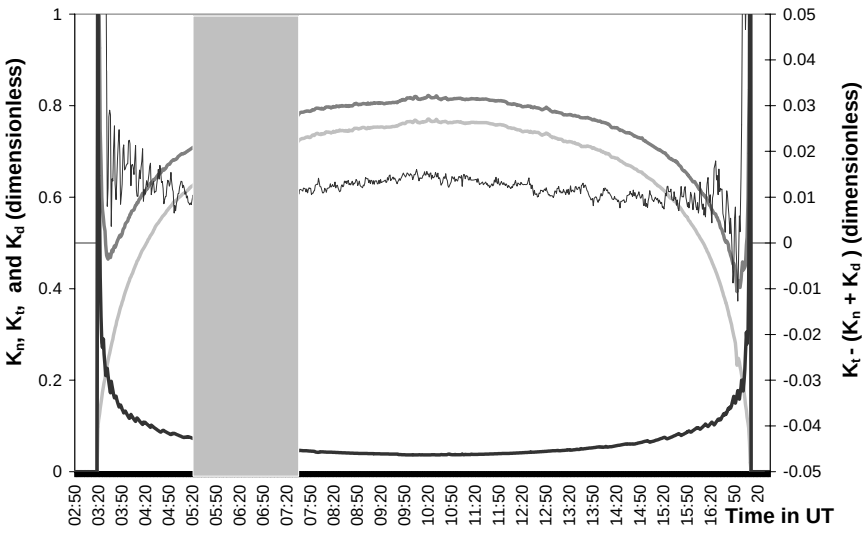

Figure 5.31 *Time-series for K_t (light grey), K_n (dark grey), K_d (thick black), and K_t – (K_n + K_d) (thin black). Eclipse time is shaded.*

In Figure 5.31, each time-series marks the eclipse with a clear indentation. Unlike the 2001 eclipse, K_t – (K_n + K_d) now shows a clear indentation, indicating that this parameter is less conservative for the 2002 eclipse than the 2001 eclipse.

The K_n versus K_t scatter diagram (Figure 5.32) shows an indication between K_t = 0.58 ; K_n = 0.45 and K_t = 0.83 ; K_n = 0.78 that a disturbance took place. This feature is also present in Figure 5.13 (eclipse 2001) but not as prominent. Keep in mind that Figure 5.32 contains more datapoints than Figure 5.13 (2001 eclipse) since the 2002 eclipse occurred on a summer (longer) day.

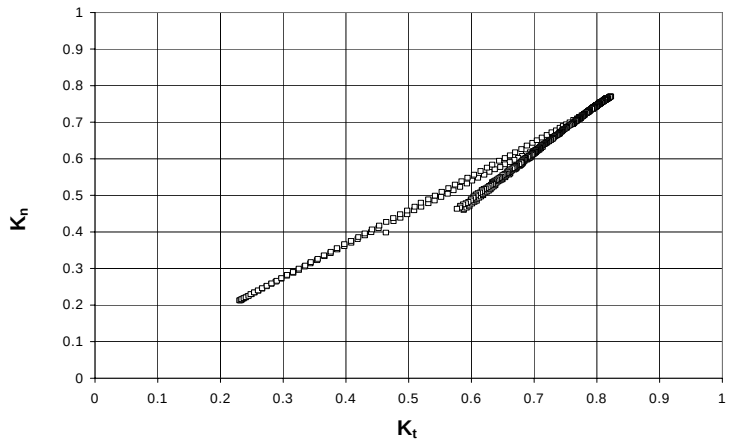

Figure 5.32 *Scatter diagram of K_n versus K_t for 4 December 2002.*

5.4.4.3 Focus on LW elements

In Section 5.3.4.3, time-series of the three terms of Equation 3.4, as well as LWD, were discussed. In this Section, a similar discussion for the 2002 eclipse is conducted. Keep in mind that eclipse day 2002 was a clear summer day. Therefore, it is expected to resemble Figure 3.7 and the associated description.

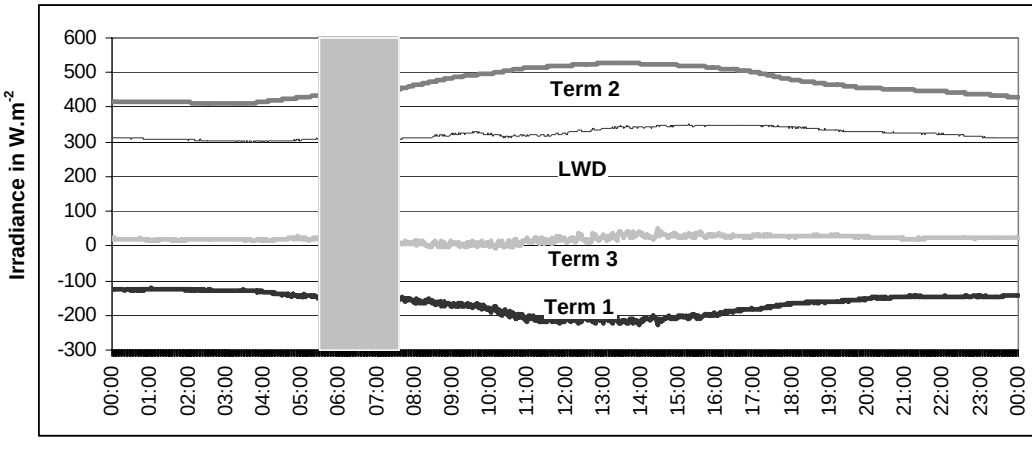

Figure 5.33 *Time-series of LWD and terms of Equation 3.4 for 4 December 2002. Eclipse time is shaded.*

Figure 5.33 shows time-series of LWD, as well as the three terms of Equation 3.4 (the pyrgeometer equation). Term 2 is mirrored to a large extent by Term 1 and Term 3 is relatively small. This leads to LWD having a small diurnal variation. Like in Figure 5.14 (the 2001 eclipse), all time-series in the shaded area (during eclipse) are not noticeably different from those outside the eclipse, therefore eclipse 2002 also had no noticeable effect on LWD.

In Figure 5.34, only the LWD data for eclipse 2002 was plotted, using a different scale. Eclipse time is shaded. Figure 5.34 does not show the same smooth diurnal pattern that Figure 5.15 exhibited. Roughly 1 hour after sunrise, LWD increases, just like in Figure 5.15. The lack of an effect of sunset on LWD in Figure 5.34 is the same as in Figure 5.15. However, no effect is seen after solar noon. The diurnal maximum LWD is 351 $W.m^{-2}$ and the minimum is 300 $W.m^{-2}$.

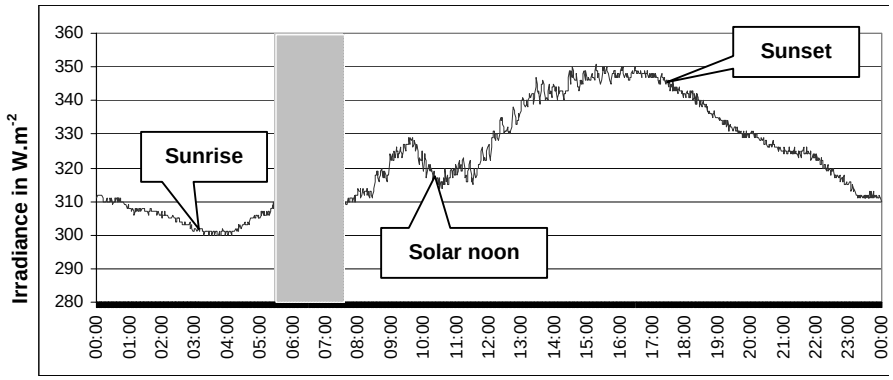

Figure 5.34 *Time-series of only LWD, for 4 December 2002. Eclipse time is shaded.*

The eclipse (shaded area) makes a small impact on LWD, which is explored in Figure 5.35.

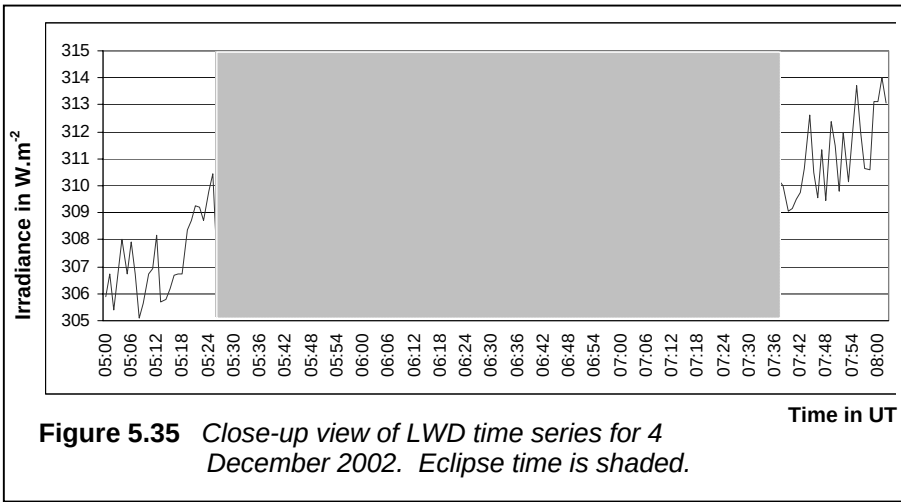

Figure 5.35 *Close-up view of LWD time series for 4 December 2002. Eclipse time is shaded.*

In Figure 5.35, a clear change in LWD can be observed during the eclipse, which could be attributed to the eclipse. At about 06:07 UT, 40 minutes after first contact (start of eclipse), LWD starts decreasing until roughly 07:12 UT, 45 minutes after maximum eclipse. It should be remembered, that these times represent an early morning, therefore LWD is expected to be in a rising trend. This explicit pattern in LWD during the eclipse, is not displayed in the corresponding time-series of eclipse 2002 (Figure 5.16).

5.4.4.4 Non-radiation measurements

Time-series of 5-minute surface (Stevenson Screen) temperature and relative humidity from the co-located AWS are shown in Figure 5.36, indicating definite features of the eclipse.

The steady temperature rise of about 2°C per hour since sunrise (03:15 UT), is halted by the eclipse, and even turned around (start of eclipse: 17.9°C; minimum in middle of eclipse: 17.5°C). This steady rise continues again after the eclipse effect starts to wane. A similar, mirrored feature, is expressed in the time-series of relative humidity, since it is inversely proportional to temperature within a given air mass.

Figure 5.36 *Time-series of surface temperature (thick line) and relative humidity (thin line) for eclipse 2002. Eclipse time is shaded.*

Figure 5.37 displays is a time-series of the AWS wind speed and direction. No significant change in wind speed or direction during or as a result of the eclipse.

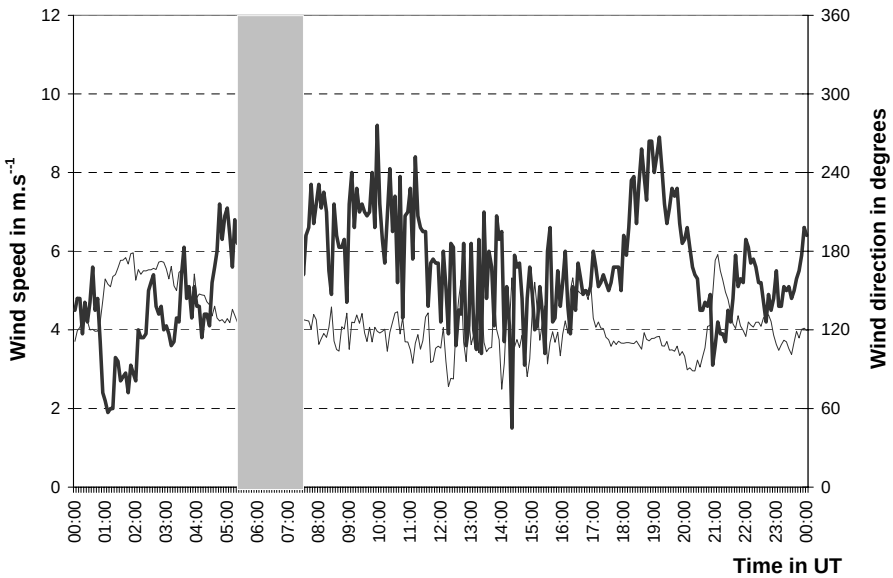

Figure 5.37 *Time-series of wind speed (thick line) and wind direction (thin line) for eclipse 2002. Time of eclipse shaded.*

5.5 CONCLUSION

The BSRN site was well placed to take maximum advantage of the clear sky conditions on both the 2001 and 2002 eclipse days, making pristine radiation measurements. This enabled the performance of analysis, as well as comparisons between the two eclipses, which were both experienced as partial eclipses at the De Aar BSRN station. There were interesting similarities, as well as differences observed for the two eclipses:

- The 2001 eclipse occurred in winter (in fact on the same day as the SH winter solstice), while the 2002 eclipse occurred in the summer (less than 3 weeks before the SH summer solstice).

- The 2001 eclipse occurred late in the afternoon, while the 2002 eclipse occurred early in the morning.

- Solar disk obscuration was comparable for both events (61% in 2001 and 73% for 2002).

- Solar elevation was comparable for both events (26° in 2001 and 40° in 2002).

- The absolute loss of radiation due to the eclipse was smaller for the 2001 eclipse than for the 2002 eclipse, but larger in relative terms.

- Background noise on OSD was comparable for both eclipses, confirming that the sky was equally clear on both days.

- Some of the expected signatures of radiation and meteorological time-series are displayed more explicitly for one eclipse than another.